

STATE OF THE CLIMATE IN 2011

Special Supplement to the
Bulletin of the American Meteorological Society
Vol. 93, No. 7, July 2012



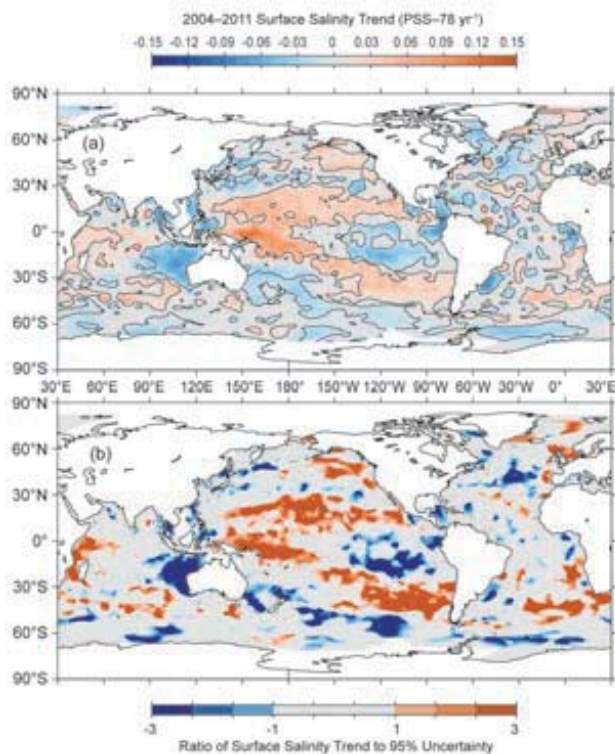


FIG. 3.13. (a) Map of local linear trends estimated from annual surface salinity anomalies for 2004–11 from Argo data (colors in PSS-78 yr⁻¹). (b) Signed ratio of the linear trend to its 95% uncertainty estimate, with increasing color intensity showing regions with increasingly statistically significant trends. White ocean areas are too data-poor to map.

f. Subsurface salinity—T. Boyer, S. Levitus, J. Antonov, J. Reagan, C. Schmid, and R. Locarnini

Mixed layer salinity and evaporation minus precipitation (E–P) are well correlated in many parts of the world’s oceans (Yu 2011). Since E–P is difficult to accurately measure over the ocean, it has been proposed that near-surface salinity could be used to constrain E–P estimates, acting as a sort of rain gauge (Schmitt 2008; Yu 2011). Durack and Wijffels (2010) have shown that E–P surface forcing has led to an intensification of the global hydrological cycle over the last 50 years, exemplified by increasing salinity at the sea surface in areas dominated by evaporation and decreasing surface salinity in areas dominated by precipitation. These surface-forced changes extend to subsurface levels. Globally-averaged near-surface waters have increased in salt content in recent times compared to long-term means, while intermediate waters have decreased in salt content (Roemmich and Gilson 2009; Helm et al. 2010). These changes can have major implications for water mass composition and circulation patterns. Investigating interannual

and long-term variability of subsurface salinity, in conjunction with sea surface salinity (SSS) and surface fluxes, can improve understanding not only of changes in the ocean, but also changes in the atmosphere affecting the global climate system.

The method used to investigate changes to subsurface salinity was to use all available subsurface ocean salinity profile data for year 2011 and construct 1° gridded fields of salinity anomalies at different depths from these data for comparison with similarly calculated fields from 2010 and the long-term mean salinity field. The majority of data used in this analysis are from the Argo profiling float program (Roemmich et al. 2009). For 2011, 121 414 Argo salinity profiles were recorded, the majority of which extend from the near surface to 2000-m depth. The geographic distribution of these data includes most of the ice-free ocean with bottom depth deeper than 2000 m. Only 14 682 of these profiles have yet undergone rigorous Argo scientific quality control because at least six months of data from the same Argo float subsequent to a profile’s date are needed for proper drift analysis. However, more than half of the non-delayed mode (real-time) data were adjusted, if necessary, based on knowledge of the salinity drift for a float that was obtained during the scientific quality control done on earlier float cycles. In addition to the Argo data, 32 662 profiles of daily averaged salinity at different depths down to 750 m from the TAO/TRITON (Pacific), PIRATA (Atlantic), and RAMA (Indian) Equatorial Ocean moored buoy arrays were included. A total of 10 274 real-time ship-based on conductivity temperature depth (CTD) salinity profiles, obtained through the Global Temperature and Salinity Profile Project (GTSP), were also used in this analysis. Data from a few additional cruises were provided by the International Council for the Exploration of the Seas (ICES), the CLIVAR program, and the New Zealand Ministry of Fisheries. A final contribution to the analysis is 30 825 salinity profiles from gliders, also obtained through GTSP. These glider data are regional, with many profiles in a limited area over a short time period. However, the geographic regions are diverse: the western North Pacific Ocean, around Australia, the Mediterranean Sea, tropical Atlantic Ocean, Gulf of Mexico, and coastal North Pacific Ocean. Additional scientific quality control was performed on all salinity and salinity anomaly data as per Boyer et al. (2009). Data from 2010 were reanalyzed to account for the increased number of delayed mode Argo data (52 124 of 112 642 profiles) and additional CTD data (4439 profiles). The 2010 fields

did not change significantly with regards to large-scale patterns from the fields used in the 2010 *State of the Climate* analysis (Levitus et al. 2011). All data and quality control flags used in the present analysis are available through the World Ocean Database (Boyer et al. 2009). All calculated fields are available at http://www.nodc.noaa.gov/OC5/3M_HEAT_CONTENT/.

The above described salinity data were analyzed as follows: Individual profiles of observed salinity were interpolated to 26 standard levels from the surface to 2000-m depth. Each standard level value was subtracted from the appropriate World Ocean Atlas (WOA; Antonov et al. 2010) long-term mean monthly salinity value for the 1° geographic grid box in which the salinity profile was taken. This removes the annual salinity cycle, leaving salinity anomaly profiles relative to the long-term mean. Salinity anomalies were bin averaged over the 1° grid boxes for each standard depth. The binned mean salinity anomalies are then objectively analyzed (Antonov et al. 2010) to generate a salinity anomaly value for each 1° ocean grid box at each standard depth from the surface to 2000 m, or the ocean bottom, whichever is encountered first. The 12 analyzed monthly salinity anomaly fields are averaged at each standard depth to produce an annual mean salinity anomaly field on a 1° global field for each depth level. This process is followed for years 2010 and 2011. The gridded 1° mean anomalies were averaged along each 1° latitude belt separately for the Atlantic, Pacific, and Indian Oceans. Zonal mean salinity anomalies for 2011 compared with the long-term mean are shown along with the zonal mean difference between salinity for 2011 and 2010. The latter give an indication of interannual change between the two years, while the former provides the context via a comparison with long-term salinity change patterns. A Student's *t* test was performed on all zonal mean anomalies at each standard depth. The mean anomalies are significant for all values > 0.1 (red and blue shading in Fig. 3.14) at the 99% level. For comparison with SSS and to understand upper ocean salinity in more detail, analyzed salinity anomaly values at each depth level in the upper 100 m for each 1° grid box were averaged using volume weighting to give a mean salinity anomaly for the upper 100 m. This mean salinity anomaly of the upper 100 meters exhibits the same

large-scale patterns of positive and negative salinity anomaly as Fig. 3.12a, with reduced amplitude.

The Pacific Ocean zonal mean salinity difference between 2011 and the long-term mean (Fig. 3.14a) reveals long-term freshening of the water column of the southern high latitudes (e.g., Böning et al. 2008) to depths > 1000 m and as far north as 35°S. Meijers et al. (2011) attribute the freshening in this area to southward movement of the Antarctic Circumpolar Current and water mass changes possibly due to increased precipitation and ice melt. There was little change in the salinity anomaly in this region from 2009 to 2010 (Levitus et al. 2011) and an increase in salinity near 60°S from 2010 to 2011 (Fig. 3.14b) illustrates the year-to-year variability about the long-term trend. The increased salinity in the upper 200 m between 40°S and the equator, interrupted by a band of freshening between 20°S and 10°S, evident in the 2011 salinity anomaly compared with the long-term mean was reinforced from 2010 to 2011, with the exception of the near surface (upper 50 m) salinity north of 10°S. Figure 3.12a (in section 3e) shows that the reason for this banding is, generally, salinification in the top 100 m in the western South Pacific and freshening in the eastern South Pacific from 40°S to the equator, with the freshening in the east weaker except in the area 20°S to 10°S. Figure 3.12a also shows very strong salinification under the SPCZ which intensified from 2010 to 2011, with salinification > 0.1 to depths of 400 m. This interannual change effectively counters the pattern of subsurface freshening propagating from the south seen between 2009 and 2010. In both

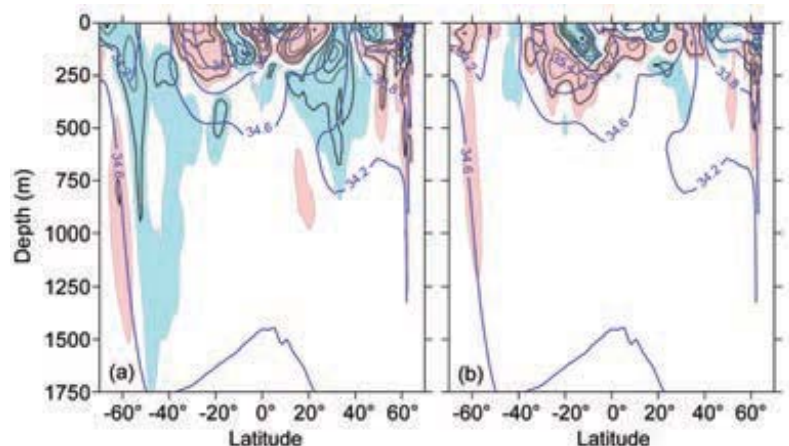


FIG. 3.14. Zonally averaged (a) 2011 salinity anomaly and (b) 2011 minus 2010 salinity field for the Pacific Ocean. Blue shading represents negative (fresh) anomalies < -0.1, red shading represents positive (salty) anomalies > 0.1. The contour interval for the anomalies is 0.2. In the background of each figure (thick blue contours) is the zonally averaged climatological mean salinity (Antonov et al. 2010). Contour intervals for the background are 0.4. All values are on the PSS.

2010 and 2011, the North Pacific was saltier in the upper 200 m than the long-term average between 20°N and 30°N (Fig. 3.14a; Levitus et al. 2011), counter to the trend shown in Boyer et al. (2005) for 1955 to 1998, and it was fresher in the main thermocline for the subtropics down to 600 m. The latter is a continuation of the trend described in Ren and Riser (2010). Except for changes in the high southern latitudes, differences between 2010 and 2011 in the Pacific were > 0.2, mainly in the upper 300 m of the water column. The salinity changes from 2009 to 2010 in the Pacific were also confined to the upper 300 m (Levitus et al. 2011).

An increase of salinity in the subtropical and tropical North Atlantic and a decrease in salinity in the subpolar North Atlantic has been described from the mid-1950s through the mid-1990s (Curry et al. 2003; Boyer et al. 2007; Wang et al. 2010). More recently, both the subpolar North Atlantic and the subtropical North Atlantic have become saltier (Boyer et al. 2007; Wang et al. 2010). The 2011 analysis (Fig. 3.15a) is consistent with these patterns. The 2011 Atlantic zonal mean salinity anomalies exhibit deep (> 500 m) large-scale increases (> 0.2) in salinity over most of the North Atlantic compared with the long-term mean. In the South Atlantic, salinification is confined mainly north of 40°S, deeper than 400 m to 30°S, reaching only to 200 m from that latitude to the equator. Freshening to depths > 500 m is found in the Atlantic, similar to the Pacific, south of 40°S. The near-surface signature of this freshening is stronger in the Atlantic than the Pacific in the high southern latitudes. The zonal mean salinity for 2011 minus 2010 shows a general year-to-year freshening across much of the Atlantic in the upper 100 m (Fig. 3.15b). Figure 3.12, section 3e, reveals a more patchy distribution of small positive and negative anomalies between the two years, with general freshening along the equator and in the western North Atlantic. The freshening along the equator extends to 300 m. Deeper down, the larger freshening that occurred between 2009 and 2010

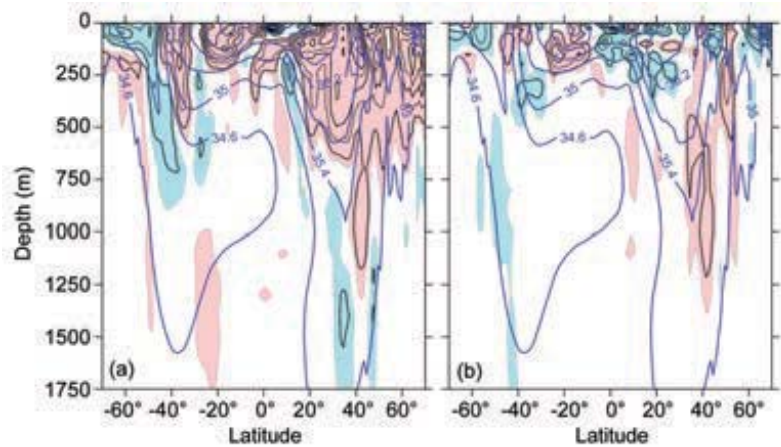


FIG. 3.15. Zonally averaged (a) 2011 salinity anomaly and (b) 2011 minus 2010 salinity field for the Atlantic Ocean. Blue shading represents negative (fresh) anomalies < -0.1, red shading represents positive (salty) anomalies > 0.1. The contour interval for the anomalies is 0.2. In the background of each figure (thick blue contours) is the zonally averaged climatological mean salinity (Antonov et al. 2010). Contour intervals for the background are 0.4. All values are on the PSS.

to 1000 m, 30°N to 40°N (Levitus et al. 2011), reversed in 2010 to 2011, with salinification > 0.2 from 500 m to > 1000 m in this area.

In the Indian Ocean, mean zonal salinity anomalies for 2011 (Fig. 3.16a) for the high southern latitudes (> 45°S) were fresher from the surface to > 1000 m than the long-term mean, except for latitudes farther south of 60°S, which were fresher only in the upper 100 m of the water column, and more saline at deeper levels. This is the same pattern seen in the Pacific

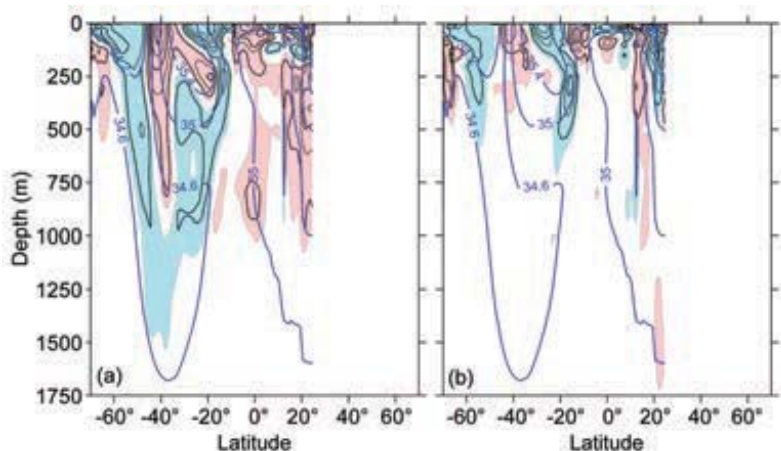


FIG. 3.16. Zonally averaged (a) 2011 salinity anomaly and (b) 2011 minus 2010 salinity field for the Indian Ocean. Blue shading represents negative (fresh) anomalies < -0.1, red shading represents positive (salty) anomalies > 0.1. The contour interval for the anomalies is 0.2. In the background of each figure (thick blue contours) is the zonally averaged climatological mean salinity (Antonov et al. 2010). Contour intervals for the background are 0.4. All values are on the PSS.

and Atlantic basins as well. The Indian Ocean was also fresher in the upper 200 m from 30°S to 10°S, and from 300 m to 1000 m in roughly the same latitude span. The latitude band from 45°S to 30°S was more saline down to 700 m, with a subsurface extension northward to almost 10°S that reaches as deep as 300 m. North of 10°S, most of the water column is more saline than the long-term mean. Much of the freshening in the Indian Ocean, outside high southern latitudes, is in the eastern Indian extending westward from the west coast of Australia (see Fig. 3.12). Comparing 2011 to 2010 (Fig. 3.16b), the freshening in the band 15°S–35°S was more intense between the two years than between 2009 and 2010 (Levitus et al. 2011), to depths of 500 m. In the western Indian Ocean, there was a large (> 0.2) increase in salinity from 20°S to the equator which is confined to the upper 200 m. In the North Indian Ocean, the eastern Arabian Sea and eastern Bay of Bengal were fresher compared to the year before (Fig. 3.12), with this freshening dominating the zonal mean salinity anomalies down to 400 m.

g. Surface currents—R. Lumpkin, G. Goni, and K. Dohan

This section describes ocean surface current changes, transports derived from ocean surface currents, and features such as rings inferred from surface currents. Surface currents are obtained from in situ and satellite (altimetry and wind) observations.

Near-surface currents are measured in situ by drogued satellite-tracked drifting buoys and by current meters on moored buoys (see Appendix 2 for specific dataset information). During 2011, the drifter array ranged in size from a minimum of 352 drogued buoys to a maximum of 576, with a median size of 416 drogued drifters (undrogued drifters continue to measure SST, but are subject to significant wind slippage; Niiler et al. 1987). The moored array included 36 buoys with current meters, all between 16°S and 21°N. These tropical moorings compose the TAO/TRITON (Pacific; 16 buoys with

current meters reporting in 2012), PIRATA (Atlantic; 6 buoys) and RAMA (Indian; 14 buoys) arrays.

Global fields of ocean currents are estimated using two methodologies, both using the AVISO Ssalto/Duacs multimission altimeter near-real time gridded product. The first is a synthesis of AVISO with in situ drifter measurements and reanalysis winds (Niiler et al. 2003), which adjusts the altimeter-derived geostrophic velocity anomalies to match the observed in situ eddy kinetic energy. The second is the purely satellite-based OSCAR (Ocean Surface Current Analyses-Real time) product, which uses AVISO altimetry, winds, SST, and the Rio05 mean dynamic topography (Rio and Hernandez 2004) to create 1/3°-resolution surface current maps averaged over the 0 m – 30 m layer of the ocean (Bonjean and Lagerloef 2002). In both cases, anomalies are calculated with respect to the time period 1992–2007. Ocean transports are derived from a combination of sea height anomaly (from altimetry) and climatological hydrography.

Global zonal current anomalies and changes in anomalies from 2010 are shown in Fig. 3.17 and discussed below for individual ocean basins.

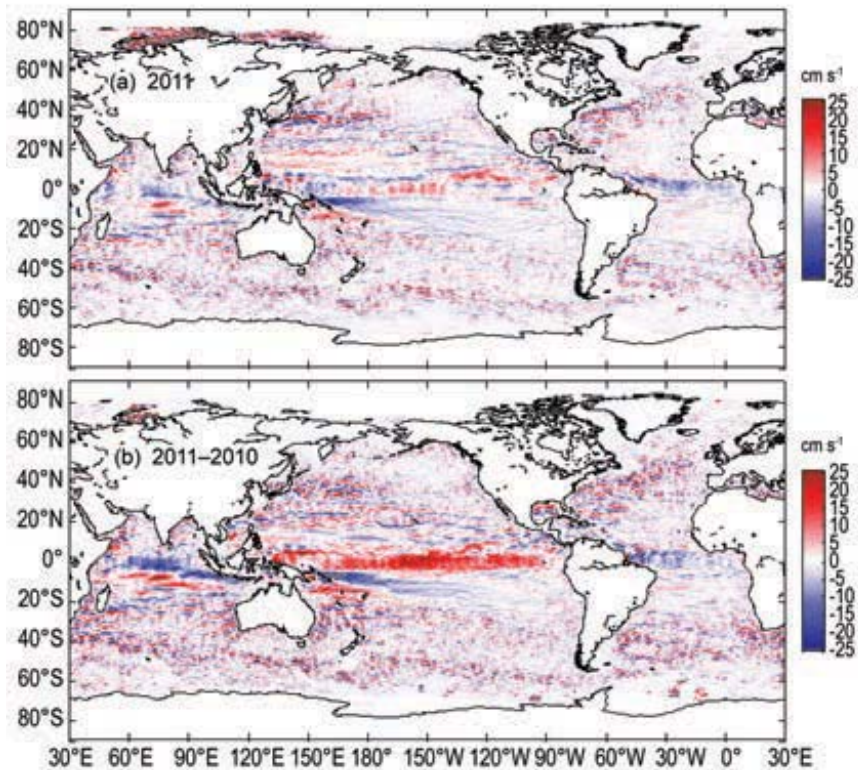


FIG. 3.17. Global zonal geostrophic anomalies (cm s^{-1}) for (a) 2011 and (b) 2011 minus 2010 derived from a synthesis of drifters, altimetry, and winds.